Scientia Iranica D (2020) 27(6), 3140–3149

Sharif University of Technology
Scientia Iranica
Transactions D: Computer Science & Engineering and Electrical Engineering
http://scientiairanica.sharif.edu

Instantaneous thrust control of linear switched reluctance motors with segmental translator

A. Zare Chavoshi and B. Ganji*

Faculty of Electrical and Computer Engineering, University of Kashan, Kashan, P.O. Box 8731753153, Iran.

Received 6 July 2018; received in revised form 22 October 2018; accepted 7 January 2019

KEYWORDS
Linear switched reluctance motor;
Segmental translator;
Thrust control;
Modeling;
Finite element method.

Abstract. The Linear Switched Reluctance Motor (LSRM) enjoys all the advantages of rotary switched reluctance machines including a simple and rugged structure, absence of magnetic material and windings on translator, high reliability, and appropriate performance over a wide range of speeds. Like the rotary switched reluctance motor with a segmental rotor, the Segmental Translator Linear Switched Reluctance Motor (STLSRM) has the capability to produce higher output power/weight than the conventional linear switched reluctance motors. Due to high advantages of the STLSRM drive, various control algorithms including current control, model predictive control, direct force control, universal control, and force distribution function are investigated for the first time to control the instantaneous thrust of this motor. By applying these algorithms to a typical three-phase STLSRM, simulation results are presented and they are compared from the force ripple reduction point of view.

1. Introduction

Due to its exclusive characteristics such as robust and simple mechanical structure, low maintenance, and high reliability and ability to work in harsh environments, Switched Reluctance Motor (SRM) can be considered as an excellent choice for various industrial applications [1–4]. Non-use of winding and permanent magnet in the rotor/translator structure has made it possible to achieve a high speed while the total weight of the motor is also reduced. However, there are some challenges that have prevented their commercial application. One of the main drawbacks of the SRM is high torque/force ripple and significant research has been completed over the last three decades to reduce it using both machine design methods [5,6] and control algorithms [7,8]. Similar to the rotary SRM, the Linear Switched Reluctance Motor (LSRM) has many benefits and the application of this motor could be limited because of its significant force ripple. In addition, using high-precision position control of the LSRM in most of motion-control industries is quite important. In the present paper, control of a special type of LSRM called Segmental Translator Linear Switched Reluctance Motor (STLSRM) using different control methods with the aim of reducing force ripple is considered.

The force control of the LSRM was proposed in [9] for the first time in which the force ripple of this motor was reduced using the multiphase excitation strategy. In [10], a simple and easy-to-implement position control method was described for high-performance motion of the LSRM in manufacturing automation. The proposed actuator has a simple structure and can be manufactured easily. In order to overcome system perturbations such as system plant parameter variations and the change of operating point, an

*. *Corresponding author.*
E-mail address: bganji@kashanu.ac.ir (B. Ganji)

doi: 10.24200/sci.2019.51380.2144

adaptive control strategy was proposed in [11] for the LSRM. A self-tuning regulator was also developed to combat uncertain control behavior of this motor. By introducing a full-order nonlinear controlled model, the robust passivity-based control was proposed in [12] for the position tracking system of the LSRM. To reduce propulsion force pulsations in the LSRM which is essential for elevators, the controlled multiphase excitation using Force Distribution Functions (FDFs) was considered in [13]. To ensure an accurate position tracking, a self-tuning regulator based on the pole-placement algorithm was developed for the LSRM in [14]. Based on the nonlinear inductance modeling, an improved force distribution function was developed in [15] for the LSRMs to minimize the force ripple. With emphasis on the functionality and practicality of the model, this study shows that the dynamic model of this motor can be derived from online estimation. Considering disturbances in the motion system, online parameter estimation using adaptive control strategy was conducted in [16] for the double-sided LSRM to determine system parameter variations and regulate control parameters in real time. Based on instantaneous control of position, speed, current, and force, a control method was introduced in [17] to reduce force ripple of the LSRM. To distribute properly the total force among the phases, a different force distribution function was also proposed in this study.

In spite of the above-mentioned researches on control of the LSRM, no work has been reported solely on control of the STLSRM, while this motor is able to produce a larger force/volume ratio [18,19]. Therefore, the main objective of the present paper is to improve the STLSRM performance using different control methods including the force control through Current Control (CC), Model Predictive Control (MPC), Direct Force Control (DFC), Universal Control (UC), and FDF method. In the following, the electromagnetic model used to predict performance of the STLSRM is described briefly in Section 2. The control algorithms proposed for the STLSRM are then explained in Section 3. By applying the proposed control methods to a typical 3-phase STLSRM, simulation results are presented in Section 4. Finally, the paper is concluded in Section 5.

2. Electromagnetic modeling

One of the serious challenges in the SRMs is the electromagnetic modeling for predicting the dynamic behavior of a motor in different operation conditions. When there is an overlap between stator/rotor poles, the saturation occurs and the characteristics of the flux-linkage will be non-linear. Due to frequent changes from linear to saturation mode, it is complicated to develop an analytical model for the SRM as already done for induction or synchronous motors. In order to investigate and implement different control methods, an exact model of the motor behavior is required. Various modeling techniques have been introduced for the SRM in the literature and they are generally categorized into: 1) linear modeling methods, 2) nonlinear modeling methods, and 3) Finite Element Method (FEM) [20,21].

2.1. The linear methods

In the linear modeling methods, behavior of the motor is expressed regardless of the impact of current on characteristics of flux- linkage and torque/force. Therefore, the effect of current on the motor's flux and inductance will be ignored in the analyses carried out by this method. In this case, the inductance is assumed to be independent of the current and it will be determined by the rotor/translator position. The main advantage of this technique is simplicity. However, the local saturation occurs in high current and therefore, the phase inductance depends on both phase current and rotor/translator position. As a result, the use of this method for modeling the dynamic characteristics of the SRM is not sufficiently accurate and the difference between simulation and experimental results is often significant.

2.2. The nonlinear methods

In the nonlinear modeling methods, both rotor/translator position and phase current are considered when obtaining the static characteristics of flux linkage with a phase. For direct torque control of the SRM, a cascade-forward back propagation neural network was used in [22] to model the nonlinear characteristic of the phase flux linkage. To implement a force distribution function method for the LSRM in [15], the nonlinear profiles of the phase inductance were expressed in terms of several mathematical equations to precisely predict behavior of the motor in different translator positions. Considering the effect of magnetic saturation, normal and propulsion forces of a planar SRM were determined in [23]. Although nonlinear modeling methods often require long and complicated calculations, they could be considered as a good alternative to linear modeling methods due to their higher accuracy.

2.3. The FEM

With advancement in computer systems, the FEM could be utilized appropriately these days for modeling and design optimization of electromagnetic devices [24,25]. In comparison to the linear and non-linear modeling methods, the FEM is more accurate because many design aspects could be considered in the modeling. However, computation time related to the FEM is longer. Various Finite Element (FE) packages such as MAXWELL, ANSYS, FLUX, and OPERA have been

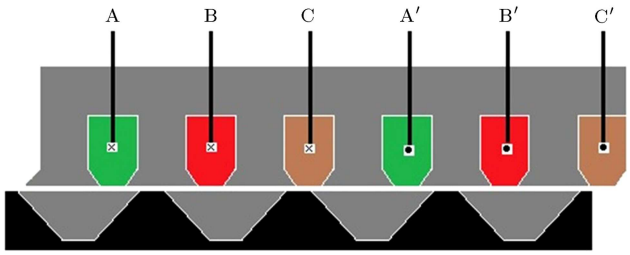

Figure 1. The Finite Element (FE) model related to a three-phase Segmental Translator Linear Switched Reluctance Motor (STLSRM) [18].

also developed for this purpose. These FE packages are built up in such a manner that different stages of modeling (creation of the geometric structure, assign attribution to various areas, meshing, determination of loads and boundary conditions, solving equations and extracting the required simulation results, etc.) can be done very easily.

Based on the FEM using ANSYS FE package, an electromagnetic simulation model has been developed here for the STLSRM, which was described elaborately in [18]. By using this simulation model, all important electromagnetic characteristics of the STLSRM including static characteristic of flux-linkage with a phase, phase current waveform, and instantaneous force could be predicted precisely. In this modeling, the geometrical model of the motor, which is illustrated for a three-phase STLSRM in Figure 1, has been created totally in ANSYS parametric design language and some critical geometrical parameters of the motor have been selected as geometrical parameters. When using the simulation model for a typical STLSRM design, one only needs to identify these geometrical parameters along with the control parameters including turn-on angle, turn-off angle, phase voltage, and speed.

3. Control methods

Different control methods considered here for the STLSRM are described in this section.

3.1. Current Control (CC)

In order to have a torque/force waveform with the least amount of ripple for the SRM, the produced force should be controlled by either direct control method or indirect control of intermediate quantities such as current and flux. In the AC motors, the reference frames are assisted to eliminate the dependence of the motor's quantities on the rotor position. Therefore, this dependency can be eliminated using transmission of motor variables to one of the reference frames. Unfortunately, there is no reference frame in the SRM to eliminate dependencies between motor variables and rotor/translator position [26]. In addition, the SRM usually operates in the saturation region because of double salient structures of the motor and consequently, the phase inductance is a function of both rotor/translator position and phase current. Therefore, studying the Current Control (CC) methods for this motor is so complicated. Since high-performance phase current tracking control is the first step in dynamic control of the LSRM drive, various strategies for CC have been introduced for the SRM. One of them is use of predetermined profiles as the reference current [27]. In this method, reference currents for generating a certain amount of force are determined by using experiment results or relying on the data obtained from FE analysis. The pulses required for the hysteresis controller are then sent to the converter for generating a special reference current. Using the predetermined profiles and hysteresis controllers with variable switching frequency is often followed by errors at high speeds, leading to oscillation and ripples in the produced torque/force waveform. In addition, the look-up tables required for these control methods must be calculated separately for each motor design. Therefore, Proportional Integral (PI) controllers with a fixed switching frequency are usually used to control the motor current.

Using the special current reference, the reference voltages were created and the motor was controlled by the Pulse Width Modulation (PWM) method in [28]. However, a linear model of the motor is required for calculation of the controller gains in this method. Due to the nonlinear flux and force characteristics, it is not easy in the SRM to calculate the controller gains. To overcome this issue in [29], the controller gains for different rotor positions between the unaligned and aligned positions are determined and stored in some look-up tables. By changing the current and rotor position using a predetermined curve in [30], the proportional integral gains simultaneously vary so that the current will follow their reference values for all situations. In [31], neural network has been used to find the gains of controller for different situations. By introducing appropriate equations in different situations in [32], the controller gains are calculated using the Bode diagram and the frequency response method. The block diagram used here to control thrust force of the STLSRM based on CC method is shown in Figure 2.

3.1.1. Model Predictive Control (MPC)

CC method based on hysteresis method has variable switching frequencies that lead to exacerbation of acoustic noises and vibration. Although PI controllers have a fixed switching frequency, these controllers increase the complexity of system and reduce the output speed response. It should be noted that a large DC bus voltage is needed to overcome the internal voltage induced at high speeds. In addition, the phase inductance should be sufficiently low to restrict large current

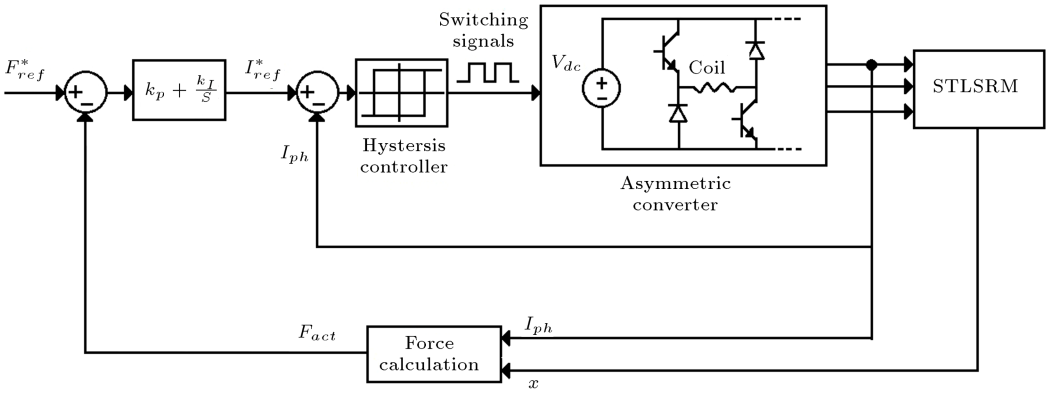

Figure 2. Block diagram for force control through current control.

variations in a short period of time. Therefore, it is a challenge to have a large DC voltage in combination with low phase inductance occurring in large-power high-speed SRM drives. The performance of high current switches will be also limited in high frequency and the hysteresis controller cannot operate effectively. On the other hand, the system cannot utilize the full control bandwidth available from converter due to poor dynamic performance and stability issues of the PI controllers. To overcome the above-mentioned challenges, the MPC method with a fixed switching frequency is suggested here. By using this method, the motor can be controlled at high speeds and large power with low-cost switches. By introducing a new method for learning and estimating the surface inductance in [33], the stochastic MPC method is used for CC of the SRM. Based on the Euler equation [34], next movement position, current, and flux linkage are calculated and the reference voltages will be obtained using the next motor parameters:

$$\frac{dx}{dt} = \frac{x(k+1) - x(k)}{T_s}, \tag{1}$$

where x is translator position and T_s is time period. The following equation can be obtained by combining Eq. (1) with the phase voltage equation:

$$V = Ri + \frac{\varphi(x_{est.k+1}, i_{ref.k+1}) - \varphi(x_k, i_k)}{x_{est.k+1} - x_k} \frac{i_{ref.k+1} - i_k}{T_s} + \frac{\varphi(x_{est.k+1}, i_{ref.k+1}) - \varphi(x_k, i_k)}{i_{ref.k+1} - i_k} \frac{i_{ref.k+1} - i_k}{T_s}, \tag{2}$$

where V is phase voltage, R phase resistance, φ flux, and $i_{ref.k+1}$ the reference current at the $k+1$ instant which is determined using the predefined current look-up table derived from the FE analysis. The main disadvantage of this method is its high dependence on the model of plant. Since the phase flux linkage of the SRM is both current and position dependent, it leads to set the nonlinear time varying state equations. The block diagram related to the suggested MPC method is shown in Figure 3.

3.2. Direct Force Control (DFC)

In the DFC method, force is directly controlled without any CC loop or FDFs. Different methods have been

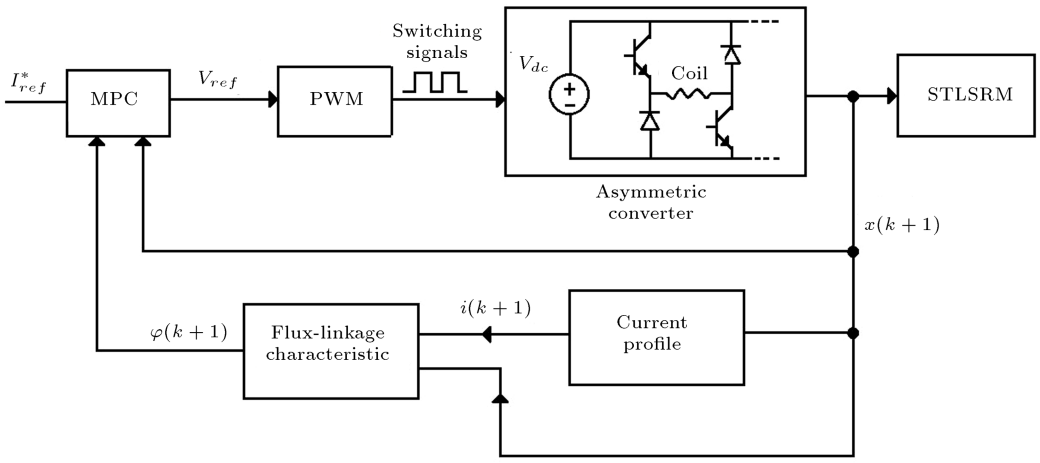

Figure 3. Block diagram for current control through the Model Predictive Control (MPC) method.

proposed for direct control of the output force in the SRM. In [35], the output force in a conventional LSRM was estimated by measuring the quantities such as the current and translator position. In order to generate the pulses required for each switch, it is compared with the reference force and it is then sent to the hysteresis controllers. Using the reference axes and voltage spatial vectors in [26,36], the torque and flux linkage are kept simultaneously in the hysteresis band. The direct torque/force control methods are very simple and torque/force ripples can be reduced without using long and complex calculations. However, the performance of DFC is limited at high speeds because the demagnetization should be performed more quickly to avoid the generator operation. Furthermore, the force sharing between different phases may not be done appropriately because there is no special emphasis on torque/force distribution among different phases. For example, one phase might have a very large current and its produced force is low while utilizing other phases can produce higher force at lower current [37]. Therefore, the switching and copper losses are increased and motor efficiency will be reduced. However, DFC at a nominal speed can significantly reduce the torque/force ripple. The structure of DFC proposed for the STLSRM is shown in Figure 4.

3.2.1. Universal Control (UC)

The requirements to introduce an attractive drive for the SRM are low torque/force ripple, operation capability over a wide speed range, maximum efficiency, balance between the switching stresses, and high-speed operation by avoiding negative torque/force production. Various control strategies have been presented for the SRM; however, each method considers some of these aspects. For example, direct control methods including hysteresis controllers are presented at a low speed. The indirect control methods such as force control through CC with PI controllers [28] and the methods based on MPC [33,34] are proposed for motor operation at a fixed switching frequency or for balancing the distribution force between each phase to achieve high-speed performance. However, current regulators cannot follow their references at high speed due to fast demagnetization. To overcome all the above-mentioned challenges, a UC method was proposed in [36] for the rotary SRM in which the DFC and CC were combined. The force produced by a phase is shown in Figure 5 in which four different regions are defined. Under the UC operation mode, DFC operation in one phase is combined with CC operation to ensure torque/force ripple minimization. In Region I, motor starts to produce the force. By starting the phase torque/force production at an earlier position, the phase advancing occurs for operation at high speeds in this region. The torque/force is produced solely by excitation of one phase in Region II. Two adjacent phases produce simultaneously the output force in Region III. In this region, the incoming phase that is operating in Region I or II produces force using DFC, while another phase that is operating in Region III produces force by CC method. The total force is the sum of DFC and the CC in the outgoing phases. Therefore, DTC is used when the phases operate in Regions I and II, while CC is used in Region III. To avoid any negative force production in Region IV, current or flux demagnetization will be taken by turning off both phase switches. By operating the incoming phase in DFC and the outgoing phase in

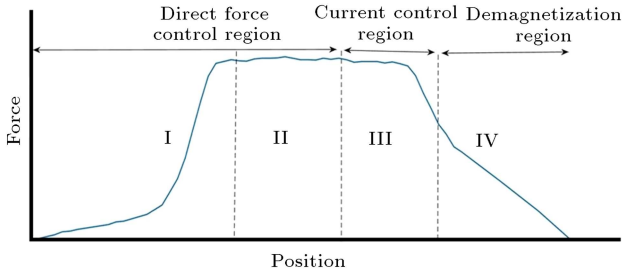

Figure 5. Regions of operation in universal control method.

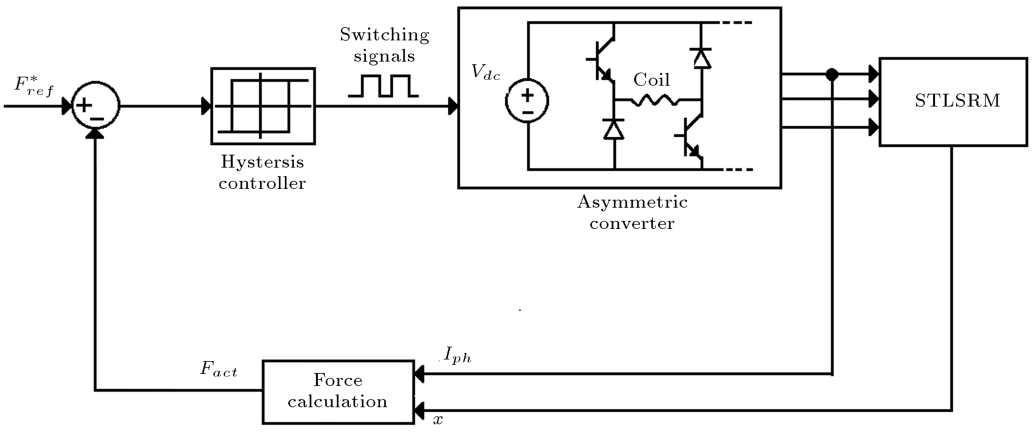

Figure 4. Block diagram for direct force control method.

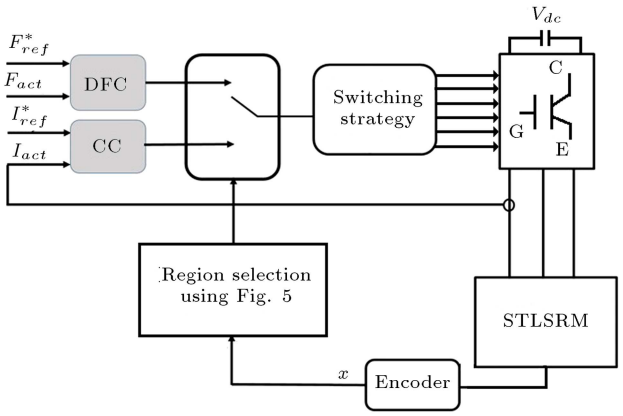

Figure 6. USC method block diagram.

CC, the problem of the DTC having complex switching is negated and if a phase cannot follow the reference force in this situation, another phase will compensate the previous phase error. The USC method block diagram is shown in Figure 6. The force required in this figure is extracted from $F - i - x$ look-up table derived from the FE analysis.

3.3. Force Distribution Function (FDF)

FDFs are known as the most effective methods for control and reduction of the torque/force ripple in the SRMs. In these functions, the reference force is distributed intelligently between two adjacent phases using simple mathematical functions to ensure that the sum of the motor output torque/force at any moment is equal to the reference force. The main objective of this method is to reduce the inherent torque/force ripple in the motor. Since the torque/force in each rotor/translator position is controlled by a special function in this method, each phase has the same contribution for the motor output force. As a result, the switching losses will be reduced due to poor distribution of force. In the distribution functions, the reference force profile is built up according to the positions of the corresponding switches phase and reference force. In this method, the reference force in each phase can be sent directly to hysteresis controllers or the reference current of each phase can be extracted using the force-current-position characteristics [13]. In the current hysteresis controller, the switching frequency is variable. When the value of the switching frequency is significant, the reference voltage can be extracted by using PI controllers and it is then utilized in the PWM method with a fixed switching frequency [38]. The choice of distribution function is not limited to a particular function and the force ripple can be reduced using different functions. The block diagram considered here to control the thrust of the STLSRM based on the force distribution functions is similar to that depicted in Figure 2 when F^*_{ref} is derived from F_{ref}, x_{on}, and x_{off} using the FDF.

To ensure that the motor will operate at the highest current-force ratio, the functions provided for controlling the motor must be evaluated using specific criteria such as the rate of changes of flux linkage or copper losses [7,39]. The distribution functions are usually divided into linear and nonlinear functions. In the linear distribution functions, the force profile of each phase will be changed linearly with the position of rotor/translator [40], while the profile will have sinusoidal [41], exponential [9], or cubic [42] variations for the nonlinear distribution functions. Due to the double salient structures of the SRM, the saturation phenomenon usually happens and therefore, torque/force ripple related to the linear functions will be greater than that for nonlinear functions [7]. Therefore, an exponential non-linear function is used in the present paper to model the operation of these functions [9]:

$$FDF(x) = \begin{cases} 0 & 0 \le x \le x_{on} \\ F_{rise}(x) & x_{on} \le x \le x_{on} + x_{ov} \\ F_{ref} & x_{on+}\, x_{ov} \le x \le x_{off} \\ F_{down}(x) & x_{off} \le x \le x_{off} + x_{ov} \\ 0 & x_{off} + x_{ov} \le x \le x_p \end{cases} \quad (3)$$

$$F_{rise}(x) = F_{ref}\left[1 - \exp\left(\frac{-(x - x_{on})^2}{x_{ov}}\right)\right], \quad (4)$$

$$F_{down}(x) = F_{ref} \exp\left(\frac{-(x - x_{off})^2}{x_{ov}}\right). \quad (5)$$

4. Simulation results

The different control methods described in Section 3 are applied to a 1 kW, 100 V, 4 m/s, 10 A 3-phase STLSRM depicted in Figure 1 with specifications given in Table 1 and the simulation results are presented here. In order to reduce the force ripple of the LSRMs, turn-on and turn-off positions play an important role. Based on the algorithm proposed in [43], these positions are determined for the discussed STLSRM. In addition, the speed of the translator for all the given simulation

Table 1. Motor specifications [18].

Stator pole width (mm)	46
Stator slot width (mm)	46
Stator pole height (mm)	67
Stator core depth (mm)	46
Air-gap length (mm)	1
Segment width (mm)	115
Translator slot width (mm)	23
Segment height (mm)	46
Core stack thickness (mm)	125
Turns per phase	160

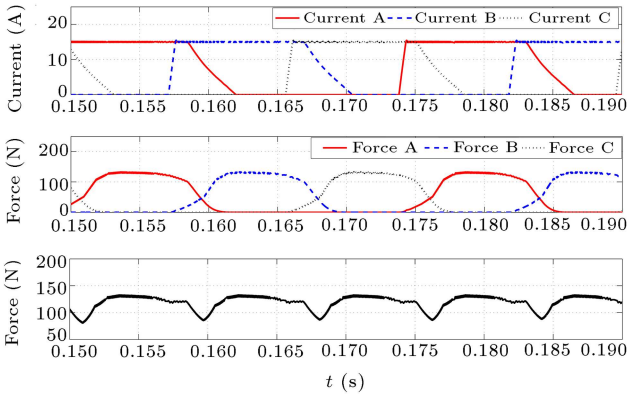

Figure 7. The phase current and thrust produced by each phase and total thrust in the current control method.

results is 4 m/s. The main purpose of the given simulation results is to evaluate the performance of all the control methods described above for the discussed 3-phase STLSRM.

Based on the CC method described in Section 3.1, the discussed STLSRM is controlled at a speed of 4 m/s and the related simulation results are presented in Figure 7. In this case, the motor is controlled without any force control loop and the main purpose is to control the motor current at a reference value of 15 A. When the force control loop is considered for the CC method, the phase current waveform, the instantaneous thrust produced by each phase and the motor output thrust are predicted and shown in Figure 8. In the CC method considering the force control loop (Figure 8), the maximum rate of thrust ripple is derived from Eq. (6) and it is 2.22%:

$$Force\ ripple = \frac{F_{inst}(\max) - F_{inst}(\min)}{F_{avg}}. \qquad (6)$$

Using the MPC algorithm described in Section 3.1.1, the discussed STLSRM is controlled for the considered operating point and the related simulation

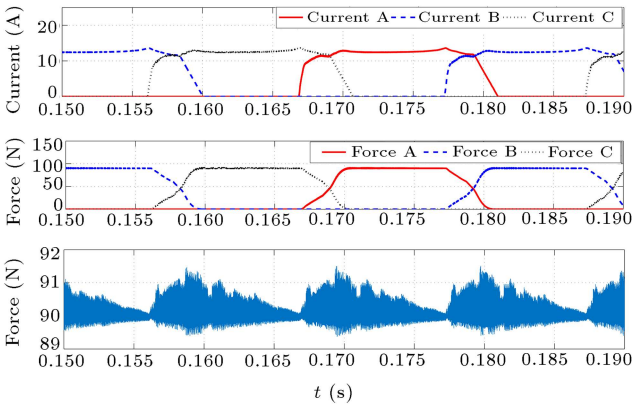

Figure 8. The simulation results related to the current control method considering the force control loop.

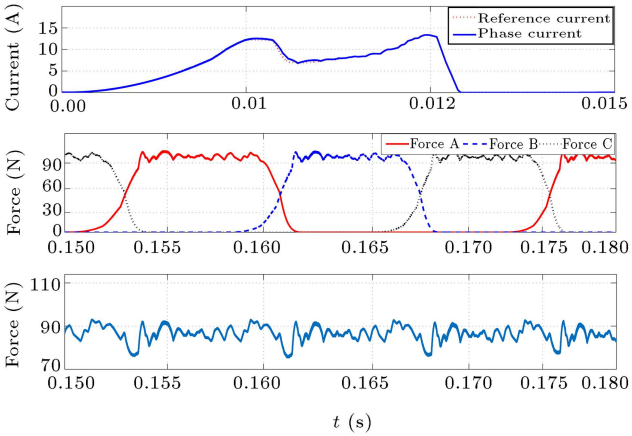

Figure 9. The reference and actual current as well as thrust produced by each phase and total thrust in the Model Predictive Control (MPC) method.

results including the reference current, actual current, the thrust produced by each phase, and instantaneous output thrust are shown in Figure 9. In this method, the predefined profiles should be used as reference current and the output thrust ripple is increased when these profiles cannot be extracted properly. For the proposed MPC method, the maximum rate of force ripple derived from Eq. (6) is about 5%.

The above-mentioned waveforms are also determined when the discussed STLSRM is controlled using the DFC method described in Section 3.2 and they are illustrated in Figure 10. Based on Eq. (6), the maximum rate of thrust ripple is derived from the output thrust waveform predicted for the DFC method and the obtained value is 3.33%.

The phase current, output force produced by one phase, and the different operation regions related to the UC method are shown in Figure 11. For the first and second regions defined in Figure 5, the motor is controlled using the pulses created by DFC method and the current controller indirectly controls the output

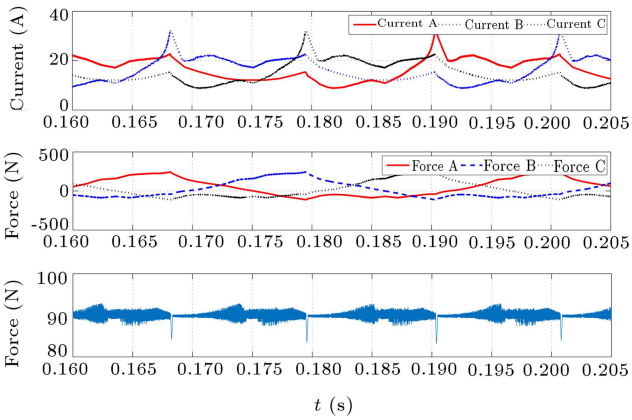

Figure 10. The phase current and thrust produced by each phase and total thrust in the direct force control method.

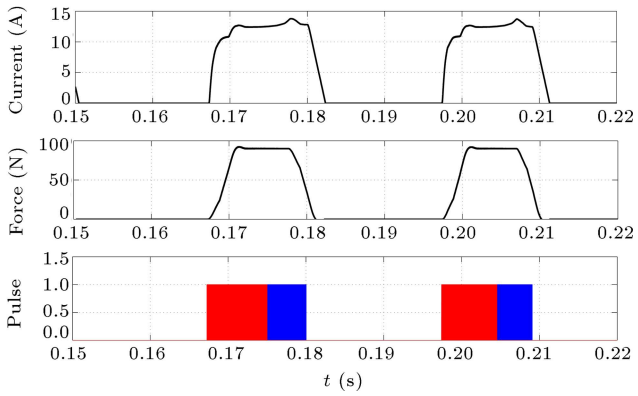

Figure 11. Output motor thrust for one phase and different operation regions in the universal control method.

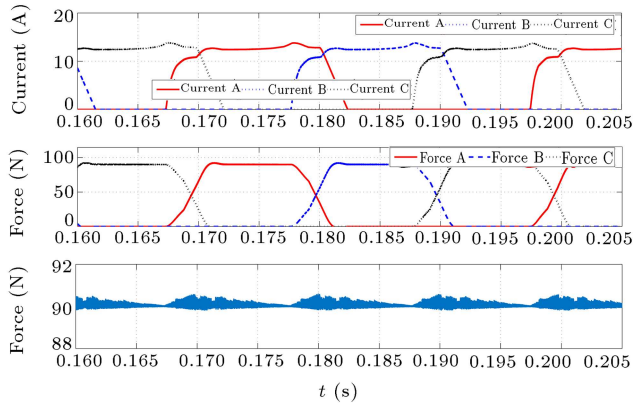

Figure 12. The phase current and total thrust in the universal control method.

force in the third region. To prevent the production of negative force (generator mode), both phase switches are turned off simultaneously in the fourth region. By applying this control method to the discussed three-phase STLSRM, the phase current waveforms and the produced thrust are predicted and they are shown in Figure 12. Based on the predicted instantaneous thrust waveform, the maximum rate of force ripple derived from Eq. (6) is 3.8%.

Based on the force distribution function method described in Section 3.3, the discussed STLSRM is controlled for the considered operating point and the related simulation results including the phase current waveforms, instantaneous thrust produced by every phase, and the output thrust waveform are predicted and shown in Figure 13. Using the predicted instantaneous output thrust, the maximum rate of force ripple is 4.2% for this control method.

For the different control methods discussed above, the force ripple percentage is calculated at different speeds and the results are shown in Figure 14. Due to the indirect control of the thrust in the CC method, the force ripple is increased at higher speeds because the hysteresis controllers cannot perform properly the magnetization. Regarding the force distribution function method, better conditions occur. However, the percentage of force ripple at low speeds is almost the same for the three methods. At low speeds, the DFC is usually used because the force ripple can be easily reduced in this method using the simple hysteresis controller. In addition, the CC method with PI controllers and new control methods such as MPC can be utilized properly at medium speeds. For higher speeds, the force distribution function method and the UC method are also appropriate choices to control the motor.

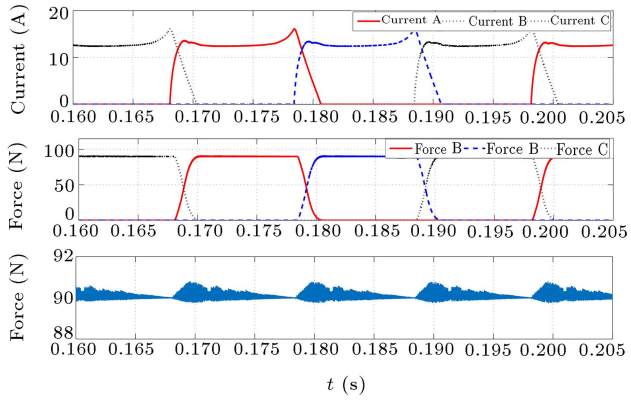

Figure 13. The phase current and thrust produced by each phase and total thrust in the force distribution function method.

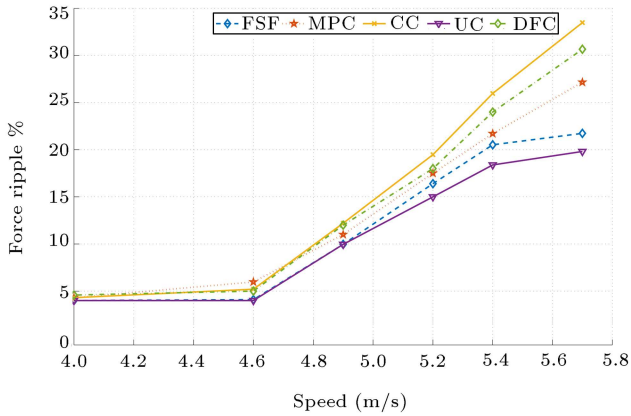

Figure 14. Force ripple in different methods at different speeds.

5. Conclusion

In order to investigate the different control methods for minimization of force ripples in the segmental translator linear switched reluctance motor, an electromagnetic simulation model based on finite element method was introduced by which all important characteristics could be predicted precisely. To control the thrust force of this motor, various control methods including current control, model predictive control, direct force control, and control using distribution

functions were described for the first time. Following the application of these proposed control algorithms to a typical 3-phase segmental translator linear switched reluctance motor, simulation results were presented and compared. Based on the simulation results given for different speeds, it was observed that the force ripple reduction was the same at low speeds for almost all of the suggested control methods. Due to the simple structure of the direct force control method, it seems that this method is more effective in terms of expenses. At the rated speed, output force ripple can be reduced effectively using the current control method and the control through the force distribution functions can significantly decrease the force ripple at higher speeds.

References

1. Todd, R., Valdivia, V., Bryan, F.J., et al. "Behavioural modelling of a switched reluctance motor drive for aircraft power systems", *IET Electr. Syst. Transp.*, **4**(4), pp. 107–113 (2014).
2. Zhu, J., Cheng, K.W.E., Xue, X., et al. "Design of a new enhanced torque in-wheel switched reluctance motor with divided teeth for electric vehicles", *IEEE Trans. Magn.*, **53**(11), 2501504 (2017).
3. Mishra, A.K. and Singh, B. "Solar photovoltaic array dependent dual output converter based water pumping using switched reluctance motor drive", *IEEE Trans. Ind. Appl.*, **53**(6), pp. 5615–5623 (2017).
4. Wang, D., Wang, X., and Du, X.F. "Design and comparison of a high force density dual-side linear switched reluctance motor for long rail propulsion application with low cost", *IEEE Trans. Magn.*, **53**(6), 7207204 (2017).
5. Sahin, C., Amac, A.E., Karacor, M., et al. "Reducing torque ripple of switched reluctance machines by relocation of rotor moulding clinches", *IET Electr. Power Appl.*, **6**(9), pp. 753–760 (2012).
6. Ma, C. and Qu, L. "Multiobjective optimization of switched reluctance motors based on design of experiments and particle swarm optimization", *IEEE Trans. Energy Convers.*, **30**(3), pp. 1144–1153 (2015).
7. Ye, J., Bilgin, B., and Emadi, A. "An offline torque sharing function for torque ripple reduction in switched reluctance motor drives", *IEEE Trans. Energy Convers.*, **30**(2), pp. 726–735 (2015).
8. Deng, X., Mecrow, B., Wu, H., et al. "Design and development of low torque ripple variable-speed drive system with six-phase switched reluctance motors", *IEEE Trans. Energy Convers.*, **33**(1), pp. 420–429 (2018).
9. Bae, H.K., Lee, B.S., Vijayraghavan, P., et al. "A linear switched reluctance motor: converter and control", *IEEE Trans. Ind. Appl.*, **36**(5), pp. 1351–1359 (2000).
10. Gan, W.C., Cheung, N.C., and Qiu, L. "Position control of linear switched reluctance motors for high-precision applications", *IEEE Trans. Ind. Appl.*, **39**(5), pp. 1350–1362 (2003).
11. Lim, H.S. and Krishnan, R. "Ropeless elevator with linear switched reluctance motor drive actuation systems", *IEEE Trans. Ind. Electron.*, **54**(4), pp. 2209–2218 (2007).
12. Zhao, S.W., Cheung, N.C., Gan, W.C., et al. "Passivity-based control of linear switched reluctance motors with robustness consideration", *IET Electr. Power Appl.*, **2**(3), pp. 164–171 (2008).
13. Lim, H.S., Krishnan, R., and Lobo, N.S. "Design and control of a linear propulsion system for an elevator using linear switched reluctance motor drives", *IEEE Trans. Ind. Electron.*, **55**(2), pp. 534–542 (2008).
14. Zhao, S.W., Cheung, N.C., Gan, W.C., et al. "High-precision position control of a linear-switched reluctance motor using a self-tuning regulator", *IEEE Trans. Power Electron.*, **25**(11), pp. 2820–2827 (2010).
15. Pan, J.F., Cheung, N.C., and Zou, Y. "An improved force distribution function for linear switched reluctance motor on force ripple minimization with nonlinear inductance modeling", *IEEE Trans. Magn.*, **48**(11), pp. 3064–3067 (2012).
16. Pan, J.F., Zou, Y., and Cao, G. "Adaptive controller for the double-sided linear switched reluctance motor based on the nonlinear inductance modeling", *IET Electr. Power Appl.*, **7**(1), pp. 1–15 (2013).
17. Masoudi, S., Feyzi, M.R., and Sharifian, M.B. "Force ripple and jerk minimisation in double sided linear switched reluctance motor used in elevator application", *IET Electr. Power Appl.*, **10**(6), pp. 508–516 (2016).
18. Ganji, B. and Askari, M.H. "Analysis and modeling of different topologies for linear switched reluctance motor using finite element method", *Alexandria Engineering Journal*, **55**, pp. 2531–2538 (2016).
19. Wang, D., Du, X., Zhang, D., et al. "Design, optimization, and prototyping of segmental-type linear switched-reluctance motor with a toroidally wound mover for vertical propulsion application", *IEEE Trans. Ind. Electron.*, **65**(2), pp. 1865–1874 (2018).
20. Krishnan, R. "Switched reluctance motor drives: modeling, simulation, analysis, design, and applications", CRC press (2001).
21. Vijayakumar, K., Karthikeyan, R., Paramasivam, S., et al. "Switched reluctance motor modeling, design, simulation, and analysis: a comprehensive review", *IEEE Trans. Magn.*, **44**(12), pp. 4605–4817 (2008).
22. Cao, G., Chen, N., Huang, S., Xiao, S., and He, J. "Nonlinear modeling of the flux linkage in 2-D plane for the planar switched reluctance motor", *IEEE Trans. Magn.*, **54**(11), Article no. 8206605 (2018).
23. Cao, G., Li, L., Huang, S., et al. "Nonlinear modeling of electromagnetic forces for the planar switched reluctance motor", *IEEE Trans. Magn.*, **51**(11), 8206605 (2015).

24. Arehpanahi, M. and Sanaei, V. "Optimal design of interior permanent magnet motor with wide flux weakening range", *Scientia Iranica*, **22**(3), pp. 1045–1051 (2015).

25. Arehpanahi, M. and Kashefi, H. "Cogging torque reduction of interior permanent magnet synchronous motor (IPMSM)", *Scientia Iranica*, **25**(3), pp. 1471–1477 (2018).

26. Cheok, D. and Fukuda, Y. "A new torque and flux control method for switched reluctance motor drives", *IEEE Trans. Power Electron.*, **17**(4), pp. 543–557 (2002).

27. Mikail, R., Husain, I., Sozer, Y., et al., "Torque ripple minimization of switched reluctance machines through current profiling", *IEEE Trans. Ind. Appl.*, **49**(3), pp. 1258–1267 (2013).

28. Shao, B. and Emadi, A. "A digital PWM control for switched reluctance motor drives", *IEEE Vehicle Power and Propulsion Conference*, Lille, France, pp. 1–6 (2010).

29. Ruiwei, Z., Xisen, Q., Liping, J., et al. "An adaptive sliding mode current control for switched reluctance motor", *IEEE Conference and Expo Transportation Electrification Asia-Pacific (ITEC Asia-Pacific)*, Beijing, country, pp. 1–6 (2014).

30. Schulz, S.E. and Rahman, K.M. "High-performance digital PI current regulator for EV switched reluctance motor drives", *IEEE Trans. Ind. Appl.*, **39**(4), pp. 1118–1126 (2003).

31. Lin, Z., Reay, D., Williams, B., et al. "High-performance current control for switched reluctance motors based on on-line estimated parameters", *IET Electr. Power Appl.*, **4**(1), pp. 67–74 (2010).

32. Ahmad, S.S. and Narayanan, G. "Linearized modeling of switched reluctance motor for closed-loop current control", *IEEE Trans. Ind. Appl.*, **52**(4), pp. 3146–3158 (2016).

33. Li, X. and Shamsi, P. "Inductance surface learning for model predictive current control of switched reluctance motors", *IEEE Trans. Transport. Electrific.*, **1**(3), pp. 287–297 (2015).

34. Mikail, R., Husain, I., Sozer, Y., et al. "A fixed switching frequency predictive current control method for switched reluctance machines", *IEEE Trans. Ind. Appl.*, **50**(6), pp. 3717–3726 (2014).

35. Pestana, L.M., Calado, M.R.A., and Mariano, S. "Direct instantaneous thrust control of 3 phase linear switched reluctance actuator", *International Conference and Exposition on Electrical and Power Engineering*, Iasi, Romania, pp. 436–440 (2012).

36. Sozer, Y., Husain, I., and Torrey, D.A. "Guidance in selecting advanced control techniques for switched reluctance machine drives in emerging applications", *IEEE Trans. Ind. Appl.*, **51**(6), pp. 4505–4514 (2015).

37. Inderka, R.B. and DeDoncker, R.W.A. "DITC-direct instantaneous torque control of switched reluctance drives", *IEEE Trans. Ind. Appl.*, **39**(4), pp. 1046–1051 (2003).

38. Xue, X.D., Cheng, K.W.E., and Ho, S.L. "Optimization and evaluation of torque-sharing functions for torque ripple minimization in switched reluctance motor drives", *IEEE Trans. Power Electron.*, **24**(9), pp. 2076–2090 (2009).

39. Gan, W., Cheung, N.C., and Li, Q. "Position control of linear switched reluctance motors for high-precision applications", *IEEE Trans. Ind. Appl.*, **39**(5), pp. 1350–1362 (2003).

40. Husain, I. and Ehsani, M. "Torque ripple minimization in switched reluctance motor drives by PWM current control", *IEEE Trans. Power Electron.*, **11**(1), pp. 83–88 (1996).

41. Ye, J., Bilgin, B., and Emadi, A. "An extended-speed low-ripple torque control of switched reluctance motor drives", *IEEE Trans. Power Electron.*, **30**(3), pp. 1457–1470 (2015).

42. Husain, I. "Minimization of torque ripple in SRM drives", *IEEE Trans. Ind. Electron.*, **49**(1), pp. 28–39 (2002).

43. Mademlis, C. and Kioskeridis, I. "Performance optimization in switched reluctance motor drives with online commutation angle control", *IEEE Trans. Energy Convers.*, **18**(3), pp. 448–457 (2003).

Biographies

Ali Zare Chavoshi received the BS degree in Electrical Engineering from Islamic Azad University of Khomeyni Shahr Branch, Iran in 2013 and the MS degree in Electrical Engineering from university of Kashan, Iran in 2016. He is currently pursuing the PhD degree at University of Esfahan and his main research interest is control of electrical machine drives.

Babak Ganji received BSc degree from Esfahan University of Technology, Iran in 2000 and MSc and PhD from University of Tehran, Iran in 2002 and 2009, respectively, all in Electrical Engineering (Power). He was granted DAAD scholarship in 2006 from Germany and worked at the Institute of Power Electronics and Electrical Drives at RWTH Aachen University as a visiting researcher for 6 months. He has been working at the University of Kashan in Iran since 2009 as an Assistant Professor and his research interest is modeling and design of advanced electric machine, especially the switched reluctance motor.